Effects of the substituted amino acid residues on the thermal properties of monomeric isocitrate dehydrogenases from a psychrophilic bacterium, *Psychromonas marina*, and a mesophilic bacterium, *Azotobacter vinelandii*

Kango Tsubouchi and Yasuhiro Takada

K. Tsubouchi
Biosystems Science Course, Graduate School of Life Science, Hokkaido University, Kita 10-jo Nishi 8-chome, Kita-ku, Sapporo 060-0810, Japan

Y. Takada (✉)
Department of Biological Sciences, Faculty of Science, Hokkaido University, Kita 10-jo Nishi 8-chome, Kita-ku, Sapporo 060-0810, Japan
E-mail: ytaka@sci.hokudai.ac.jp
Tel: +81-11-706-2742
Fax: +81-11-706-2742

Abstract A cold-adapted monomeric isocitrate dehydrogenase from a psychrophilic bacterium, *Psychromonas marina*, (*Pm*IDH) showed a high degree of amino acid sequential identity (64%) to a mesophilic one from a mesophilic bacterium, *Azotobacter vinelandii* (*Av*IDH). In this study, eight corresponding amino acid residues were substituted between them by site-directed mutagenesis, and several thermal properties of the mutated IDHs were examined. In the *Pm*IDH mutants, *Pm*L735F, substituted Leu735 of *Pm*IDH by the corresponding Phe of *Av*IDH, showed higher specific activity and thermostability of activity than wild-type *Pm*IDH, while the H600Y and N741P mutations of *Pm*IDH resulted in the decreased specific activity and thermostability of activity. On the other hand, among the *Av*IDH mutants, *Av*P718T showed lower optimum temperature and thermostability of activity than wild-type *Av*IDH. In multiple *Pm*IDH mutants variously combined the H600Y, L735F and N741P mutations, *Pm*H600YL735F, including the H600Y and L735F mutations, showed higher specific activity than *Pm*H600Y and similar optimum temperature and thermostability of activity to *Pm*H600Y. Furthermore, *Pm*L735FN741P exhibited higher specific activity and thermostability of activity than *Pm*N741P. These results indicated that the effects of the three mutations of *Pm*IDH are additive on specific activity of both *Pm*H600YL735F and *Pm*L735FN741P and on thermostability of *Pm*L735FN741P.

Keywords cold-adapted isocitrate dehydrogenase · mesophilic isocitrate dehydrogenase · site-directed mutagenesis · *Psychromonas marina* · *Azotobacter vinelandii*.

Introduction

$NADP^+$-dependent isocitrate dehydrogenase (IDH; EC 1. 1. 1. 42) is an enzyme catalyzing the oxidative decarboxylation of isocitrate to α-ketoglutarate and CO_2 with the reduction of $NADP^+$ in the TCA cycle of most bacteria. Based on the subunit composition, bacterial IDH can be classified into two types: a homodimer consisting of 40–45 kDa subunits and a single polypeptide of 80–100 kDa. Many bacteria possess only one type of IDH. Thus, *Escherichia coli* (Burke et al. 1974) and *Thermus thermophiles* (Eguchi et al. 1989) have only dimeric IDH while those of *Corynebacterium glutamicum* (Eikmanns et al. 1995) and *Vibrio parahaemolyticus* (Fukunaga et al. 1992) are monomeric. However, several bacteria such as psychrophilic bacteria, *Colwellia maris* and *Colwellia psychrerythraea* strain NRC1004, and a psychrotrophic bacterium, *Pseudomonas psychrophila*, have been known to hold both of the two type IDHs (Ochiai et al. 1979 and 1984; Maki et al. 2006; Matsuo et al. 2010). These two types of IDH catalyze the same reaction, but their amino acid sequences and immunological cross-reactivities are different from each other (Fukunaga et al. 1992; Ishii et al. 1987 and 1993; Sahara et al. 2002).

A psychrophilic bacterium, *Psychromonas marina*, isolated from sea water off the coast of the Okhotsk Sea in Japan, has only monomeric IDH (*Pm*IDH) (Kawasaki et al. 2002; Hirota et al. 2017). *Pm*IDH shows the highest activity at about 35˚C, retains 13% of the maximum activity at 10˚C, and loses over 70% of the activity after incubation for 10 min at 30˚C, indicating that this IDH is a cold-adapted enzyme. In this way, cold-adapted enzymes generally show high catalytic activity at low temperatures and marked thermolability (Siddiqui and Cavicchioli 2006). These properties of the cold-adapted enzymes are ascribable to their enhanced structural flexibility, allowing them for easy binding of the substrates to

their active sites at low temperatures and rapid conformational changes for the catalysis without energy loss (Gerdey et al. 1997; Fields and Somero 1998). On the other hand, a mesophilic nitrogen-fixing bacterium, *Azotobacter vinelandii*, also possesses only one monomeric IDH (*Av*IDH) (Sahara et al. 2002; Chung and Franzen 1969). However, *Av*IDH is mesophilic and retains over 90% of the activity after incubation for 10 min at 45˚C, and the optimum temperature for activity is about 50˚C (Yoneta et al. 2004; Watanabe et al. 2005). Since amino acid sequence of *Pm*IDH shows a high degree of identity to that of *Av*IDH (64%), their structures are suggested to resemble each other. The three-dimensional structure and active site of *Av*IDH have been determined by the crystallographic analysis (Yasutake et al. 2002 and 2003), and this enzyme has been found to contain domain I, consisting of the N-terminal region 1 and the C-terminal region 3, and domain II corresponding to the intermediate region 2. Furthermore, the active site is located at the interface of the two domains, and the amino acid residues involved in the binding of isocitrate, metal ion and $NADP^+$ are dispersedly present in all three regions of the IDH protein. The molecular model of *Pm*IDH is shown in Fig.1a. Previous studies indicate that C-terminal regions 3 is involved in the thermal properties (e.g. optimum temperature for activity and thermostability) of this class of enzymes (Hirota et al. 2017; Watanabe et al. 2005).

In this study, to identify the amino acid residues implicated in the thermal properties of *Pm*IDH and *Av*IDH, the substitutional mutations of their several amino acid residues located in the region 3 were introduced into the IDH genes by site-directed mutagenesis, and their thermal properties of the mutated IDHs overproduced in the *E. coli* cells were investigated.

Materials and Methods

Bacteria, plasmids and growth media

E. coli DEK2004 (Thorsness and Koshland 1987), which is a mutant defective in IDH, was used as a host for expression of the mutated *Pm*IDH and *Av*IDH genes. The plasmid vector pTrcHisB (Invitrogen) was used to confer the N-terminal $(His)_6$-tag on the expressed proteins. The plasmids pHis*Pm*IDH (Hirota et al. 2017) and pHis*Av*IDH (Watanabe et al. 2005), carrying the *Pm*IDH and *Av*IDH genes, respectively, in the *Bam*HI-*Sac*I site of pTrcHisB, were used as templates for PCR in site-directed mutagenesis. *E. coli* transformants were cultivated with vigorous shaking in Luria-Bertani (LB) medium (Sambrook and Russell 2001) or Super broth medium (Watanabe et al. 2005). If necessary, ampicillin and tetracycline were added to the culture media at concentrations of 0.1 mg/ml and 0.015 mg/ml, respectively.

Construction of the mutated IDH genes by site-directed mutagenesis

As previously reported (Kurihara and Takada 2012), mutated *Pm*IDH and *Av*IDH genes were constructed by three times PCR (Supplementary Fig. S1). The reaction mixture (50 µl) contained 50 ng of pHis*Av*IDH, pHis*Pm*IDH or both products of the first and second PCRs as template, 15 pmol forward and reverse primers shown in Supplementary Tables S1 and S2, respectively) and 1 U KOD-Plus-Neo DNA polymerase (TOYOBO) in the buffer prepared by the manufacturer. Since the codons for Asn741 of *Pm*IDH and Pro739 of *Av*IDH are located at the 3'-terminal of each IDH gene, the full lengths of the mutated IDH genes were amplified by only once PCR in the same reaction mixture (50 µl) as the first PCR,

except that primer D' or H' (Supplementary Tables S1 and S2, respectively) was used as the reverse primer to introduce the substitution of amino acid residue of *Pm*IDH and *Av*IDH. Each PCR was carried out for 30 cycles under the conditions shown in Supplementary Tables S3 and S4 in a Veriti 96 well Thermal cycler (Applied Biosystems). The final PCR products were digested with *Bam*HI and *Sac*I and then ligated into the *Bam*HI-*Sac*I site of pTrcHisB with Ligation-Convenience Kit (Nippon Gene). The plasmids carrying the mutated IDH genes were transformed into the *E. coli* DEK2004 cells by a calcium chloride method (Sambrook and Russell 2001). Introduction of the mutation was confirmed by DNA sequencing of the plasmids with Big Dye Terminator v3.1 Cycle Sequencing Kit (Applied Biosystems) and a sequencer, 3130 genetic Analyzer (Applied Biosystems). Double and triply mutated *Pm*IDH genes were constructed as described above, except that the plasmids carrying the singly mutated *Pm*IDH genes were used as template.

Overexpression and purification of His-tagged IDHs

E. coli DEK2004 transformed with pTrcHisB carrying *Pm*IDH, *Av*IDH or their mutated IDH genes was grown at 37˚C with shaking in 1 liter of Super broth medium until OD_{600} of the culture reached 0.8–1.0. The culture was rapidly cooled for 30 min on ice, and 1 mM isopropyl-β-D-thiogalactopyranoside was added to the culture. Then, the culture was further incubated at 15˚C for 18-24 h to induce the overexpression of the His-tagged IDH. The subsequent purification of the IDH proteins by Ni-NTA agarose (Qiagen) column chromatography were carried out as described previously (Hirota et al. 2017). The final eluate of chromatography was concentrated with polyethylene glycol #6,000 and then

dialyzed against 20 mM sodium phosphate buffer (pH 8.0), containing 2 mM $MgCl_2$, 300 mM NaCl, 5 mM sodium citrate, 1 mM dithiothreitol (DTT) and 50% (v/v) glycerol. All purified IDHs were stored at -30˚C until use. SDS-polyacrylamide gel electrophoresis (SDS-PAGE) of the purified IDH proteins was performed with 10% gel at 120 V by the method of Laemmli (1970).

Enzyme assay

The IDH activity was assayed at various temperatures as described previously (Ochiai et al. 1979). The reaction mixture (2 ml) contained 33 mM Tris-HCl (pH 8.0), 0.67 mM $MnCl_2$, 0.12 mM $NADP^+$, 2 mM sodium isocitrate and an appropriate amount of enzyme. For the assay of the wild-type and mutated *Pm*IDHs, 0.15 M NaCl was added to the reaction mixture. Before the enzyme assay, the wild-type and mutated *Pm*IDHs and *Av*IDHs were diluted with 20 mM sodium phosphate buffer (pH 8.0), containing 2 mM $MgCl_2$, and 1 mM DTT to a final concentration of 10–40 μg and 4–14 μg protein/ml, respectively, except that *Pm*IDH replaced His600 by Tyr (*Pm*H600Y) was diluted with the above buffer containing 10% (v/v) glycerol to a concentration of 30–85 μg protein/ml. To examine thermostability of the IDH activity, the purified IDHs were dialyzed overnight at 4˚C against 20 mM sodium phosphate buffer (pH 8.0) containing 2 mM $MgCl_2$, 0.3 M NaCl, 10% (v/v) glycerol and 1 mM DTT. After incubation for 10 min at various temperatures, the enzymes were immediately cooled on ice for 10 min, and the residual activities were then assayed at 30˚C. One unit of IDH activity was defined as the amount capable of catalyzing the reduction of 1 μmol $NADP^+$ per 1 min. Protein concentration was assayed by the method of Lowry et al. (1951) with bovine serum albumin as a standard. All data for activity are the

mean values ± SD of duplicate assays from at least two independent experiments.

Results

Construction and purification of mutated IDHs

Multiple amino acid sequence alignment of the C-terminal region 3 in various cold-adapted and mesophilic monomer-type IDHs revealed that several amino acid residues at the corresponding positions are different among them (Fig. 1). Such amino acid residues were expected to be determinants of their different thermal properties. Thus, the following eight amino acid residues located at the corresponding positions were substituted between *Pm*IDH and *Av*IDH. In the previous study on the substitutional mutations of the corresponding amino acid residues, it was elucidated that Pro709 of *Av*IDH and Ala711 of *Cm*IDH, and Pro739 of the former and Ala741 of the latter are involved in their catalytic activity and thermostability of activity, respectively, and particularly Pro718 of *Av*IDH and Ala720 of *Cm*IDH markedly contribute to both the thermal properties and catalytic activity (Kurihara and Takada 2012). The Pro709, Pro718 and Pro739 of *Av*IDH corresponded to Ala711, Thr720 and Asn741 of *Pm*IDH. On the other hand, as well as *Cm*IDH, the monomeric IDH of *C. psychrerythraea* NRC1004 (*Cp*IDH) is also cold-adapted, but the latter catalytic activity is much less than the former one (Maki et al. 2006). Yasuda et al. (2013) and Kobayashi and Takada (2014) reported that Phe735 of *Cm*IDH and the corresponding Leu735 of *Cp*IDH are involved in their different catalytic activity and thermostability of activity. The corresponding amino acid residues is Leu in *Pm*IDH but is Phe in *Av*IDH (Fig. 1). Furthermore, among different amino acid residues between the

mesophilic and the cold-adapted IDHs, amino acid residues with different properties (such as charge, hydrophobicity and so on), namely Ala626, His600, Met667 and Thr678 of *Pm*IDH and the corresponding Pro624, Tyr598, Leu665 and Glu676 of *Av*IDH, were also selected.

The *Pm*IDH mutants substituted His600, Ala626, Met667, Thr678, Ala711, Thr720, Leu735 and Asn741 by the corresponding Tyr598, Pro624, Leu665, Glu676, Pro709, Pro718, Phe733 and Pro739 of *Av*IDH were termed *Pm*H600Y, *Pm*A626P, *Pm*M667L, *Pm*T678E, *Pm*A711P, *Pm*T720P, *Pm*L735F and *Pm*N741P, respectively. In contrast, the counterpart *Av*IDH mutants were *Av*Y598H, *Av*P624A, *Av*L665M, *Av*E676T, *Av*P709A, *Av*P718T, *Av*F733L and *Av*P739N. The *Av*P709A gene constructed previously (Kurihara and Takada 2012) was used in this study. SDS-PAGE of the final eluates of Ni-NTA column chromatography revealed that all wild-type and mutated *Pm*IDHs and *Av*IDHs with molecular masses of about 80 kDa were purified almost to homogeneity (Supplementary Figs. S2 and S3). It has been reported that His-tagging at the N-terminals of *Pm*IDH and *Av*IDH has no significant effect on their thermal properties (Hirota et al. 2017; Watanabe et al. 2005; Kurihara and Takada 2012).

Temperature-dependence of wild-type and mutated *Pm*IDH activities

To examine the effect of the substituted amino acid residues on the catalytic function of *Pm*IDH, the wild-type and mutated IDH activities were assayed at various temperatures (Figs. 2 and 3a). Furthermore, the optimum temperatures for their activities (T_{opt}) and the specific activities at 10˚C and the respective optimum temperatures are summarized in Table 1. Since the purified *Pm*H600Y was unstable and the activity was completely lost by the dilution with the buffer

without glycerol used for the other IDHs, the purified sample of *Pm*H600Y was diluted with the buffer containing 10% glycerol before the enzyme assay as described in Materials and Methods, and the activity was compared with that of the wild-type *Pm*IDH diluted with the same buffer. The T_{opt} of wild-type *Pm*IDH (*Pm*WT) appeared to be between 35 and 40˚C, and the enzyme retained 26% of the maximum activity at 10˚C. The specific activities of the mutated *Pm*IDH at 10˚C were comparable to that of *Pm*WT except for higher and lower activities of *Pm*L735F and *Pm*H600Y, respectively. *Pm*A711P, *Pm*T720P, and *Pm*L735F showed slightly higher T_{opt} (40˚C) and higher specific activities at 45˚C than *Pm*WT. Particularly, *Pm*L735F was the most active variant. In contrast, the T_{opt} of *Pm*H600Y was 30˚C, and this mutant and *Pm*N741P exhibited much lower specific activities than *Pm*WT. However, the two mutants retained higher relative activities at lower temperatures between 10˚C and 30˚C than the other *Pm*IDHs. On the other hand, temperature-dependence of the *Pm*A626P, *Pm*M667L and *Pm*T678E activities were similar to that of *Pm*WT.

Thermostability of wild-type and mutated *Pm*IDH activities

After incubation for 10 min at various temperatures, the residual activities of the wild-type and mutated *Pm*IDHs were assayed at 30˚C to evaluate thermostability of wild-type and mutated *Pm*IDH activities (Figs. 3b and 4). By incubation at 25˚C, 64% of the *Pm*WT activity was lost, and temperature at which 50% of the activity was lost by incubation for 10 min ($t_{½}$) was 23.6˚C. On the other hand, the residual activities of *Pm*A626P, *Pm*T678E, *Pm*A711P, *Pm*T720P and *Pm*L735F at the same temperature were slightly higher than *Pm*WT, and their $t_{½}$ values were 25.6˚C, 26.4˚C, 26.2˚C, 24.7˚C and 27.5˚C, respectively (Table 1). Among them,

*Pm*L735F exhibited the highest residual activity (78%) after the same incubation. These results indicate that the five IDH mutants, particularly *Pm*L735F, are slightly more thermostable than *Pm*WT. In contrast, *Pm*N741P and *Pm*H600Y showed lower residual activities than *Pm*WT and lost 90% and 32% of the activities after incubation at 25˚C, and the $t_{½}$ values were 21.2˚C and 26.5˚C, respectively. Since *Pm*WT diluted with the buffer containing 10% glycerol almost completely retained its activity after the same incubation and showed the $t_{½}$ value of 28.3˚C (Fig. 3b), *Pm*H600Y and *Pm*N741P were found to be more thermolabile than *Pm*WT.

Temperature-dependence of wild-type and mutated *Av*IDH activities

As shown in Fig. 5, the wild-type *Av*IDH (*Av*WT) showed the maximum activity (465 unit/mg protein) at 55˚C (Table 2), and its activity was much higher than that of *Pm*WT. At 10˚C, the enzyme exhibited 10% of the maximum activity (specific activity of 49 unit/mg protein). The T_{opt} of the six *Av*IDH mutants, *Av*P624A, *Av*L665M, *Av*E676T, *Av*P709A, *Av*F733L and *Av*P739N, were the same as that of *Av*WT, while *Av*Y598H and *Av*P718T exhibited slightly lower T_{opt} (50–55˚C) than *Av*WT. In addition, *Av*P718T showed obviously lower specific activity above 35˚C than those of *Av*WT, and the activity at temperatures between 55 and 60˚C were the lowest of all mutated *Av*IDH. On the other hand, the relative activities of all mutated *Av*IDHs at 10˚C were analogous to that of *Av*WT (9.4–12.0%) except for slightly higher activity of *Av*P718T (14%).

Thermostability of wild-type and mutated *Av*IDH activities

*Av*WT completely retained its activity after incubation at 40˚C, the residual activity after incubation at 45˚C was 78% (Fig 6), and its $t_{½}$ value was 47.5˚C (Table 2). The residual activities of *Av*P718T after incubation at 40˚C and 45˚C were 91% and 42%, respectively, and the $t_{½}$ value was 44.2˚C. These results indicate that *Av*P718T is more thermolabile than *Av*WT. On the other hand, the other mutated *Av*IDHs showed similar thermostability to *Av*WT, and their $t_{½}$ values were 47.1–48.2˚C.

Kinetic parameters of mutated *Pm*IDHs and *Av*IDHs

The values of K_m for isocitrate, k_{cat} and k_{cat}/K_m in the wild-type *Pm*IDH and *Av*IDH and their mutants, *Pm*H600Y, *Pm*L735F, *Pm*N741P and *Av*P718T, of which thermal properties were significantly different from those of the respective wild-type IDHs, at 20˚C are summarized in Table 3. The catalytic efficiency, k_{cat}/K_m, of *Pm*L735F was about 1.5-fold higher than that of *Pm*WT because of its decreased K_m and increased k_{cat} values. In contrast, *Pm*N741P and *Pm* H600Y showed the decreased k_{cat}/K_m values, due to the about two-fold higher K_m value than *Pm*WT in the former mutant and both three-fold higher K_m and lower k_{cat} values than *Pm*WT in the latter one. On the other hand, *Av*WT showed much higher k_{cat}/K_m value than *Pm*WT, and the k_{cat}/K_m value of *Av*P718T was equivalent to that of *Av*WT.

Construction and purification of double and triple *Pm*IDH mutants

To elucidate the effects of the combined substitutions of amino acid residues on the thermal properties of *Pm*IDH, based on the above results, the multiple mutations of H600Y, L735F and N741P were introduced to the *Pm*IDH gene. The multiple *Pm*IDH mutants were termed *Pm*H600YL735F (His600 and Leu735 of *Pm*IDH were substituted by the corresponding Tyr and Phe of *Av*IDH, respectively), *Pm*H600YN741P, *Pm*L735FN741P and *Pm*H600YL735FN741P. These His-tagged IDH mutants overexpressed in the *E. coli* cells were purified. From SDS-PAGE of final eluates of Ni-NTA column chromatography, *Pm*H600YL735F and *Pm*L735FN741P were confirmed to be almost homogeneously purified (lanes 2 and 4 in Supplementary Fig. S4, respectively). However, the purification of *Pm*H600YN741P and *Pm*H600YL735FN741P was unsuccessful because of slight amounts of about 80 kDa protein band (lanes 3 and 5 in Supplementary Fig. S3, respectively). In fact, the maximum specific activities of the two mutants were very low (6.9 unit/mg protein at 25˚C and 8.4 unit/mg protein at 30˚C, respectively).

Thermal properties and kinetic parameters of multiple *Pm*IDH mutants

The T_{opt} of *Pm*L735FN741P was the same as that of *Pm*WT (Fig. 7a). Furthermore, its specific activity was comparable to that of *Pm*WT (Table 1). After incubation for 10 min at 20˚C, *Pm*L735FN741P exhibited higher residual activity (80%) than *Pm*N741P (63%), but lower than *Pm*L735F (100%) and *Pm*WT (87%) (Fig. 7b), and its $t_{½}$ value was 22.7˚C, an intermediate between those of *Pm*L735F (27.5˚C) and *Pm*N741P (21.2˚C), suggesting that *Pm*L735FN741P is more thermostable and thermolabile than *Pm*N741P and *Pm*L735F, respectively. On the other hand, *Pm*H600YL735F showed similar T_{opt} and thermostability (the $t_{½}$ value of 27 ˚C)

to *Pm*H600Y, but its specific activity was higher at all temperatures tested than that of *Pm*H600Y (Fig. 3).

The K_m value of *Pm*H600YL735F was about two-fold higher and lower than those of *Pm*WT and *Pm*H600Y, respectively (Table 3). The k_{cat}/K_m value of *Pm*H600YL735F was about two-fold higher than that of *Pm*H600Y. On the other hand, the K_m value of *Pm*L735FN741P was lower and higher than that of *Pm*N741P and *Pm*WT, respectively, while its k_{cat} value was almost the same as that of *Pm*WT.

Discussion

As reported previously (Watanabe et al. 2005), the mesophilic *Av*IDH showed high specific activities at low temperatures such as 10˚C rather than the cold-adapted *Pm*IDH, implying that the thermolability of the enzyme proteins is not necessary for high catalytic activity at low temperatures. On the other hand, in cold-active and thermostable superoxide dismutases from psychrophilic *Pseudoalteromonas haloplanktis* and *Euplotes focardii*, their cold activities were suggested to be achieved by the increased local flexibility of their active sites (Merllino et al. 2010; Pischedda et al. 2018). This mechanism might be explaining the activity of *Av*IDH at low temperatures.

*Pm*L735F exhibited the highest specific activity below 45˚C and thermostability of all mutated *Pm*IDHs and slightly increased T_{opt}, indicating that Leu735 of *Pm*IDH is involved in the catalytic activity and thermostability of activity. Similar results were obtained in the substitutional mutant of Leu735 of the cold-adapted *Cp*IDH by Phe (Yasuda et al. 2013). In the molecular model of *Pm*L735F (Fig. 8a), the side chains of Phe735 and Phe663 are located closely (the

distance between the two side chains of 5 Å). A pair of aromatic side chains in protein with a distance between phenyl ring centroids of 4.5–7 Å can form an aromatic-aromatic interaction, contributing to the stabilization of protein structure, and thermophilic proteins tend to form more interactions than mesophilic counterparts (Burley and Petsko 1985; Kannan and Vishveshwara 2000). Therefore, such an aromatic-aromatic interaction between Phe663 and Phe735 may cause the increased thermostability of the *Pm*L735F activity. However, since no change of thermostability of activity was observed in the corresponding F733L mutation in *Av*IDH regardless of the resultant deletion of aromatic-aromatic interaction, further experiments, including the substitutions of Phe663 of *Pm*IDH by another amino acids, are needed to elucidate the involvement of this interaction.

*Pm*H600Y showed much lower specific activities at all temperatures tested and thermostability of activity than wild-type *Pm*IDH. Furthermore, this IDH mutant was so unstable that no activity was detected by the dilution with the buffer without 10% glycerol used for other IDHs. These results suggest that His600 of *Pm*IDH contributes to its catalytic activity and thermostability of activity. Tyr598 of *Av*IDH and the corresponding His600 of *Pm*IDH are located near the respective Arg600 and Arg602 (Fig. 1). This Arg of *Av*IDH is a recognition site for $NADP^+$ (Yasutake et al. 2003). Furthermore, Tyr600 can form additional two hydrogen bonds between Leu656 and Ser650 in *Pm*H600Y (Fig. 8b). Since Ser650 is adjacent to Arg651, another recognition site of $NADP^+$, these hydrogen bonds may affect the recognition and binding of $NADP^+$ and result in the decreased activity and stability of *Pm*IDH. On the other hand, this mutation is also thought to interfere with the global stability of the protein.

Although only slight shift-up of T_{opt} and thermostability of activity were observed in *Pm*A711P and *Pm*T720P, the *Pm*N741P mutation made *Pm*IDH more thermolabile and resulted in the decreased activity above 20˚C. Since N atom in

main chain of Pro is included in its side chain and forms a ring structure, the rotation of N-Cα bond in backbone of polypeptide chain is restricted (Schimmel and Flory 1968; MacArthur and Thornton 1991). So, Pro is considered to decrease the flexibility of protein structure and increase the stability (Suzuki et al. 1987; Suzuki 1989) Therefore, the substitution by Pro does not always contribute to the increase of thermostability of activity and, sometimes, even make it thermolabile. In fact, similar results were obtained in the substitution of Ala741 of *Cm*IDH, corresponding to Asn741 of *Pm*IDH, by Pro (Kurihara and Takada 2012).

The N741P mutation increase only the K_m value, and the H600Y mutation results in the decreased k_{cat} and the increased K_m values (Table 3). A local rigidity of region far from the catalytic site was reported to be involved in catalytic activity of the cold-adapted elastase (Papaleo et al. 2006), and Asn741 of *Pm*IDH is so. Furthermore, the thermolability of the cold-adapted enzymes derived from their high structural flexibility has been thought to increase the K_m values because of a poor binding to the ligand (Fields et al. 2015). Therefore, the high K_m values of *Pm*H600Y and *Pm*N741P may result from their high thermolability.

Among the *Av*IDH mutants, *Av*P718T showed the decreased T_{opt}, specific activity at high temperatures and thermostability of activity, indicating that this mutation makes *Av*IDH more thermolabile. Similar results were reported in the substitution of Pro718 of *Av*IDH by Ala (Kurihara and Takada 2012). These indicate that Pro718 of *Av*IDH is necessary to the high specific activity and thermostability of activity. As shown in Fig. 8c, the distances from Thr718 to Ile712 and Gly714 in *Av*P718T (5.29 Å and 4.81 Å, respectively) are longer than those from Pro718 to Ile712 and Gly714 in the wild-type *Av*IDH (5.01 Å and 4.71 Å, respectively). However, Thr718 can form an additional hydrogen bond to Thr723. Although hydrogen bond is generally known to contribute to the protein stability (Vogt and Argos 1997; Pace et al. 2014), the extended space among

Ile712, Gly714 and Thr718 and the loss of Pro residue in *Av*P718T by the mutation may be more effective on the thermal property of *Av*IDH than the additional hydrogen bond.

*Pm*L735FN741P, combined the L735F and N741P mutations, showed higher specific activity and higher thermostability of activity than *Pm*N741P, but lower than wild-type *Pm*IDH (Fig. 7), indicating that the L735F mutation improves the specific activity and thermostability of *Pm*N741P but the effect of the N741P mutation is larger than that of the L735F one. Similar results were also obtained in *Pm*H600YL735F (Fig. 3). In this case, the effect of the L735F mutation appears to be smaller than the H600Y one. In the previous study on the cold-adapted *Cp*IDH, the effects of the combined F693L, Q724L and L735F mutations, which result in the increased activity and thermostability of activity, were reported to be additive (Kobayashi and Takada 2014). Thus, similar additive effects were observed in the *Pm*H600YL735F and *Pm*L735FN741P mutations in this study.

References

Arnold K, Bordoli L, Kopp J, Schwede T (2006) The SWISS-MODEL Workspace: A web-based environment for protein structure homology modelling. Bioinformatics 22:195–201

Biasini M, Bienert S, Waterhouse A, Arnold K, Studer G, Schmidt T, Kiefer F, Cassarino TG, Bertoni M, Bordoli L, Schwede T (2014) SWISS-MODEL: modelling protein tertiary and quaternary structure using evolutionary information. Nucl Acids Res 42:W252–W258

Burke WF, Johanson RA, Reeves HC (1974) $NADP^+$-specific isocitrate dehydrogenase of *Escherichia coli*. II. Subunit structure. Biochim Biophys Acta 351:333–340

Burley SK, Petsko GA (1985) Aromatic-aromatic interaction: a mechanism of protein structure stabilization. Science 229:23–28

Chung AE, Franzen JS (1969) Oxidized triphosphopyridine nucleotide specific isocitrate dehydrogenase from *Azotobacter vinelandii*. Isolation and characterization. Biochemistry 8:3175–3184

Eguchi H, Wakagi T, Oshima T (1989) A highly stable NADP-dependent isocitrate dehydrogenase from *Thermus thermophilus* HB8: purification and general properties. Biochim Biophys Acta 990:133–137

Eikmanns BJ, Rittmann D, Sahm H (1995) Cloning, sequence analysis, expression, and inactivation of the *Corynebacterium glutamicum icd* gene encoding isocitrate dehydrogenase and biochemical characterization of the enzyme. J Bacteriol 177:774–782

Fields PA, Dong Y, Meng X, Somero GN (2015) Adaptations of protein structure and function to temperature: there is more than one way to ‘skin a cat’. J Exp Biol 218:1801–1811

Fields PA, Somero GN (1998) Hot spots in cold adaptation: localized increases in conformational flexibility in lactate dehydrogenase A4 orthologs of Antarctic notothenioid fishes. Proc Natl Acad Sci USA 95:11476-11481

Fukunaga N, Imagawa S, Sahara T, Ishii A, Suzuki M (1992) Purification and characterization of monomeric isocitrate dehydrogenase with $NADP^+$-specificity from *Vibrio parahaemolyticus* Y-4. J Biochem 112:849–855

Gerdey C, Aittaleb M, Arpigny JL, Baise E, Chessa JP, Garsoux G, Petrescu I, Feller G (1997) Psychrophilic enzymes: a thermodynamic challenge. Biochim Biophys Acta 1342:119-131

Guex N, Peitsch MC, Schwede T (2009) Automated comparative protein structure modeling with SWISS-MODEL and Swiss-PdbViewer: A historical perspective. Electrophoresis 30:S162–S173

Hirota R, Tsubouchi K, Takada Y (2017) $NADP^+$-dependent isocitrate dehydrogenase from a psychrophilic bacterium, *Psychromonas marina*. Extremophiles 21:711–721

Ishii A, Ochiai T, Imagawa S, Fukunaga N, Sasaki S, Minowa O, Mizuno Y, Shiokawa H (1987) Isozymes of isocitrate dehydrogenase from an obligately psychrophilic bacterium, *Vibrio* sp. strain ABE-1: purification, and modulation of activities by growth conditions. J Biochem 102:1489–1498

Ishii A, Suzuki M, Sahara T, Takada Y, Sasaki S, Fukunaga N (1993) Genes encoding two isocitrate dehydrogenase isozymes of a psychrophilic bacterium, *Vibrio* sp. strain ABE-1. J Bacteriol 175:6873–6880

Kannan N, Vishveshwara S (2000) Aromatic clusters: a determinant of thermal stability of thermophilic proteins. Protein Eng 13:753–761

Kawasaki K, Nogi Y, Hishinuma M, Nodasaka Y, Matsuyama H, Yumoto I (2002) *Psychromonas marina* sp. Nov., a novel halophilic, facultatively psychrophilic bacterium isolated from the coast of the Okhotsk Sea. Int J Syst Evol

Microbiol 52:1455–1459

Kiefer F, Arnold K, Künzli M, Bordoli L, Schwede T (2009) The SWISS-MODEL Repository and associated resources. Nucl Acids Res 37:D387–D392

Kobayashi M, Takada Y (2014) Effects of the combined substitutions of amino acid residues on thermal properties of cold-adapted monomeric isocitrate dehydrogenases from psychrophilic bacteria. Extremophiles 18:755–762

Kurihara T, Takada Y (2012) Analysis of the amino acid residues involved in the thermal properties of the monomeric isocitrate dehydrogenases of the psychrophilic bacterium *Colwellia maris* and the mesophilic bacterium *Azotobacter vinelandii*. Biosci Biotechnol Biochem 76:2242–2248

Laemmli UK (1970) Cleavage of structural proteins during the assembly of the head of bacteriophage T4, Nature 227:680–685

Lowry OH, Rosebrough NJ, Farr AL, Randall RJ (1951) Protein measurement with the Folin phenol reagent. J Biol Chem 193:144–148

MacArthur MW, Thornton JM (1991) Influence of proline residues on protein conformation. J Mol Biol 218:397–412

Maki S, Yoneta M, Takada Y (2006) Two isocitrate dehydrogenases from a psychrophilic bacterium, *Colwellia psychrerythraea*. Extremophiles 10:237–249

Matsuo S, Shirai H, Takada Y (2010) Isocitrate dehydrogenase isozymes from a psychrotrophic bacterium, *Pseudomonas psychrophila*. Arch Microbiol 192:639–650

Merlino A, Krauss IR, Castellano I, Vendittis E, Rossi B, Conte M, Vergara A, Sica F (2010) Structure and flexibility in cold-adapted iron superoxide dismutases: The case of the enzyme isolated from *Pseudoalteromonas haloplanktis*. J Struct Biol 172:343-352

Ochiai T, Fukunaga N, Sasaki S (1979) Purification and some properties of two

NADP$^+$-specific isocitrate dehydrogenases from an obligately psychrophilic marine bacterium, *Vibrio* sp., strain ABE-1. J Biochem 86:377–384

Ochiai T, Fukunaga N, Sasaki S (1984) Two structurally different NADP$^+$-specific isocitrate dehydrogenases in an obligately psychrophilic bacterium, *Vibrio* sp. strain ABE-1. J Gen Appl Microbiol 30:479–487

Pace CN, Fu H, Fryar KL, Landua J, Trevino SR, Schell D, Thurlkill RL, Imura S, Scholtz JM, Gajiwala K, Sevcik J, Urbanikova L, Myers JK, Takano K, Hebert EJ, Shirley BA, Grimsley GR (2014) Contribution of hydrogen bonds to protein stability. Protein Sci 23:652– 661

Papaleo E, Riccardi L, Villa C, Fantucci P, Gioia LD (2006) Flexibility and enzymatic cold-adaptation: a comparative molecular dynamics investigation of the elastase family. Biochim Biophys Acta 1764:1397–1406

Pettersen EF, Goddard TD, Huang CC, Couch GS, Greenblatt DM, Meng EC, Ferrin TE (2004) UCSF Chimera–a visualization system for exploratory research and analysis. J Comput Chem 25:1605–1612

Pischedda A, Ramasamy KP, Mangiagalli M, Chiappori F, Milanesi L. Miceli C, Pucciarelli S, Lotti M (2018) Antarctic marine ciliates under stress: superoxide dismutases from the psychrophilic *Euplotes focardii* are cold-active yet heat tolerant enzymes. Sci Rep 8:14721

Robert X, Gouet P (2014) Deciphering key features in protein structures with the new ENDscript server. Nucl Acids Res 42:W320–W324

Sahara T, Takada Y, Takeuchi Y, Yamaoka N, Fukunaga N (2002) Cloning, sequencing, and expression of a gene encoding the monomeric isocitrate dehydrogenase of the nitrogen-fixing bacterium, *Azotobacter vinelandii*. Biosci Biotechnol Biochem 66:489–500

Sambrook J, Russell D (2001) Molecular cloning: a laboratory manual, 3rd ed. Cold spring Harbor Laboratory, Cold spring Harbor, N.Y.

Schimmel PR, Flory PJ (1968) Conformational energies and configurational statistics of copolypeptides containing L-proline. J Mol Biol 34:105–120

Siddiqui KS, Cavicchioli R (2006) Cold-adapted enzymes. Annu Rev Biochem 75:403-433

Suzuki Y (1989) A general principle of increasing protein thermostability. Proc Jpn Acad Ser B Phys Biol Sci 65:146–148

Suzuki Y, Oishi K, Nakano H, Nagayama T (1987) A strong correlation between the increase in number of proline residues and the rise in thermostability of five *Bacillus* oligo-1,6-glucosidases. Appl Microbiol Biotechnol 26:546–551

Thorsness PE, Koshland DE Jr (1987) Inactivation of isocitrate dehydrogenase by phosphorylation is mediated by the negative charge of the phosphate. J Biol Chem 262:10422–10425

Vogt G, Argos P (1997) Protein thermal stability: hydrogen bonds or internal packing? Fold Des 2:S40–46

Watanabe S, Yasutake Y, Tanaka I, Takada Y (2005) Elucidation of stability determinants of cold-adapted monomeric isocitrate dehydrogenase from a psychrophilic bacterium, *Colwellia maris*, by construction of chimeric enzymes. Microbiology 151:1083–1094

Yasuda W, Kobayashi M, Takada Y (2013) Analysis of amino acid residues involved in cold activity of monomeric isocitrate dehydrogenase from psychrophilic bacteria, *Colwellia maris* and *Colwellia psychrerythraea*. J Biosci Bioeng 116:567–572

Yasutake Y, Watanabe S, Yao M, Takada Y, Fukunaga N, Tanaka I (2002) Structure of the monomeric isocitrate dehydrogenase: evidence of a protein monomerization by a domain duplication. Structure 10:1637–1648

Yasutake Y, Watanabe S, Yao M, Takada Y, Fukunaga N, Tanaka I (2003) Crystal structure of the monomeric isocitrate dehydrogenase in the presence of

NADP$^+$. J Biol Chem 278:36897–36904

Yoneta M, Sahara T, Nitta K, Takada Y (2004) Characterization of chimeric isocitrate dehydrogenases of a mesophilic nitrogen-fixing bacterium, *Azotobacter vinelandii*, and a psychrophilic bacterium, *Colwellia maris*. Curr Microbiol 48:383–388

Legend to figures

Fig. 1 Molecular model of *Pm*IDH (a) and alignment of amino acid sequences of region 3 in monomeric IDHs from various bacteria (b). (**a**) The model of *Pm*IDH was built with the program SWISSPDB VIEWER (http://www.expasy.org/spdbv), using the *Av*IDH (PDB no. 1ITW) as a homology model. The regions 1, 2 and 3 are indicated by orange, blue and purple, respectively. (**b**) The amino acid sequences of region 3 in monomeric IDHs from *A. vinelandii* (AvIDH; DNA database accession no. D73443), *P. psychrophila* (PpIDH; AB425997), *C. maris* (CmIDH; D14047), *C. psychrerythraea* strain 34H (Cp34HIDH; CP000083), *C. psychrerythraea* NRC1004 (CpIDH; AB174851) and *P. marina* (PmIDH) (AB795036). The black and gray bars show two mesophilic and four cold-adapted IDHs, respectively. The area surrounded by line represents the region 3 of these IDHs. Identical and similar amino acids of the IDHs are showed by red boxes and by red letters, respectively. The secondary structures, α-helix and β-sheet, of *Av*IDH are depicted above the alignment by coil and arrow, respectively. The numbers over and under the alignment indicate the positions of amino acid residues from the N-terminal of the two mesophilic and four cold-adapted IDHs, respectively. The arrows show the amino acid residues involved in the recognition and binding of $NADP^+$ in *Av*IDH. The stars indicate the positions of amino acid residues substituted in this study. Letters surrounded by green lines indicate the amino acid residues substituted in previous studies (see text). This figure and secondary structure of *Av*IDH (PDB no. 1ITW) was made with a program ESPrinpt ver 3.0 (Robert and Gouet 2014).

Fig. 2 Effect of temperature on the activities of wild-type and mutated *Pm*IDHs. *Pm*WT (◆), *Pm*A626P (△), *Pm*M667L (□), *Pm*T678E (●), *Pm*A711P (■),

*Pm*T720P (×), *Pm*L735F (◇) and *Pm*N741P (▲) are indicated. (**b**) Relative activities are represented as percentages of the maximum activity of each enzyme.

Fig. 3 Effects of temperature on the activities (a, b) and the thermostability (c) of wild-type *Pm*IDH, *Pm*H600Y and *Pm*H600YL735F. *Pm*WT (◆), *Pm*H600Y (○) and *Pm*H600YL735F (□) are indicated. (**b**) Relative activities are represented as percentages of the maximum activity of each enzyme. (**c**) Residual activities assayed at 30˚C after incubation for 10 min at various temperatures are represented as percentages of those without incubation. Before the enzyme assay, the three IDHs were diluted with the buffer containing 10% glycerol (see Materials and Methods).

Fig. 4 Thermostability of wild-type and mutated *Pm*IDH activities. Residual activities assayed at 30˚C after incubation for 10 min at various temperatures are represented as percentages of those without incubation. Symbols are the same as Fig. 2.

Fig. 5 Effect of temperature on the activities of wild-type and mutated *Av*IDHs. *Av*WT (◆), *Av*Y598H (○), *Av*P624A (△), *Av*L665M (□), *Av*E676T (●), *Av*P709A (■), *Av*P718T (×), *Av*F733L (◇) and *Av*P739N (▲) are indicated. (**b**) Relative activities are represented as percentages of the maximum activity of each enzyme.

Fig. 6 Thermostability of wild-type and mutated *Av*IDH activities. Residual activities assayed at 30˚C after incubation for 10 min at various temperatures are represented as percentages of those without incubation. Symbols are the same as Fig. 5.

Fig. 7 Effects of temperature on the activities (a, b) and the thermostability (c) of wild-type *Pm*IDH and its single and double mutants. *Pm*WT (◆), *Pm*L735F (◇), *Pm*N741P (▲) and *Pm*L735FN741P (○) are indicated. (**b**) Relative activities are represented as percentages of the maximum activity of each enzyme. (**c**) Residual activities assayed at 30˚C after incubation for 10 min at various temperatures are represented as percentages of those without incubation.

Fig. 8 Molecular models of wild-type and mutated IDHs. Molecular models around the 735th amino acid residues of *Pm*WT and *Pm*L735F (**a**), around the 600th amino acid residues of *Pm*WT and *Pm*H600Y (**b**) and around the 718th amino acid residues of *Av*WT and *Av*P718T (**c**) are indicated. The models of *Pm*WT, *Av*WT and their mutants were built with the program SWISS-MODEL, using the *Av*IDH (PDB no. 1ITW) as a template model (Arnold et al. 2006; Guex et al. 2009; Biasini et al. 2014; Kiefer et al. 2009). (**a, c**) The red dash lines indicate the interatomic distance. (**b, c**) The blue lines indicate the hydrogen bonds. The figures of IDH structures were prepared with the program UCSF Chimera (Pettersen et al. 2004).

(a)

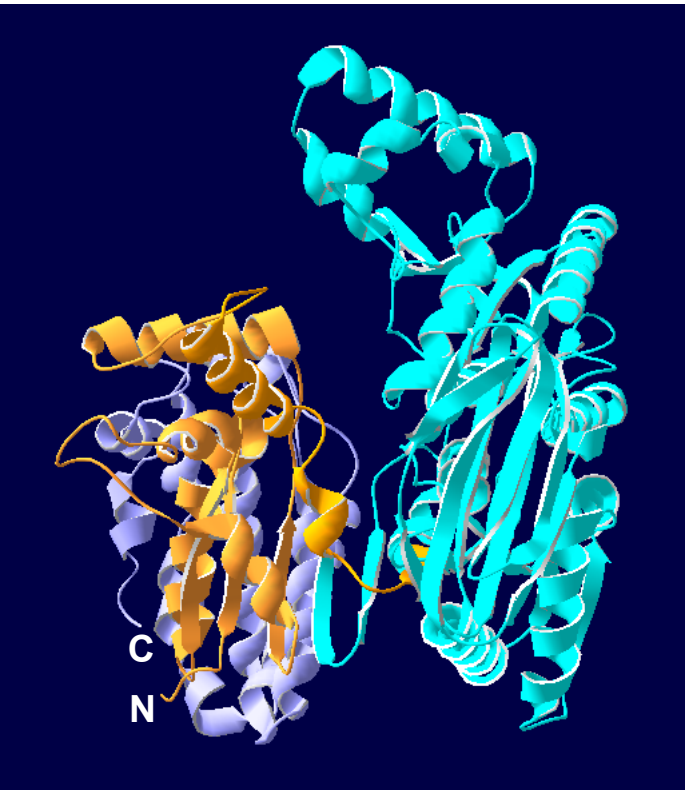
C
N

(b)

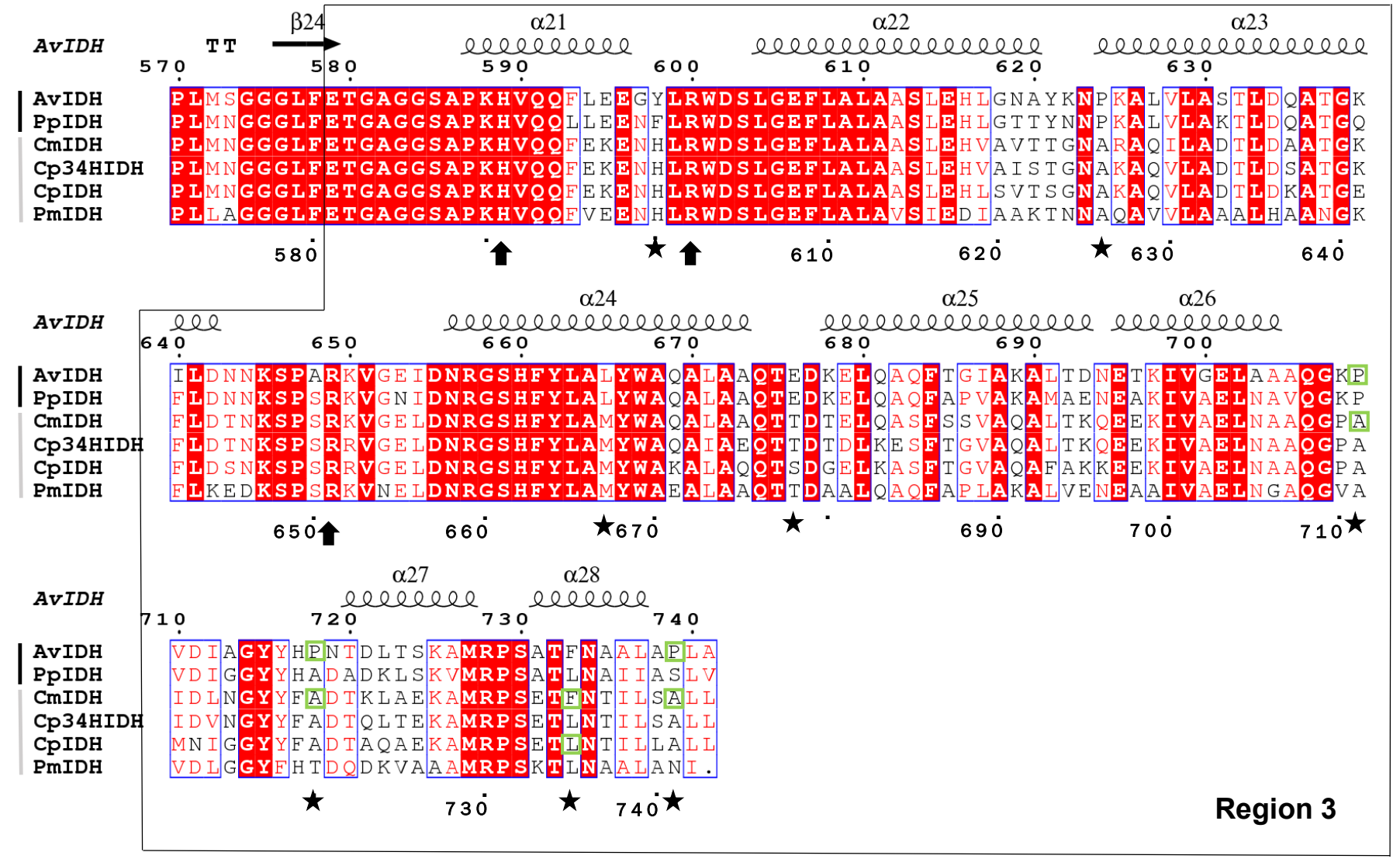
AvIDH
PpIDH
CmIDH
Cp34HIDH
CpIDH
PmIDH
β24
α21
α22
α23
α24
α25
α26
α27
α28
Region 3

Fig. 1

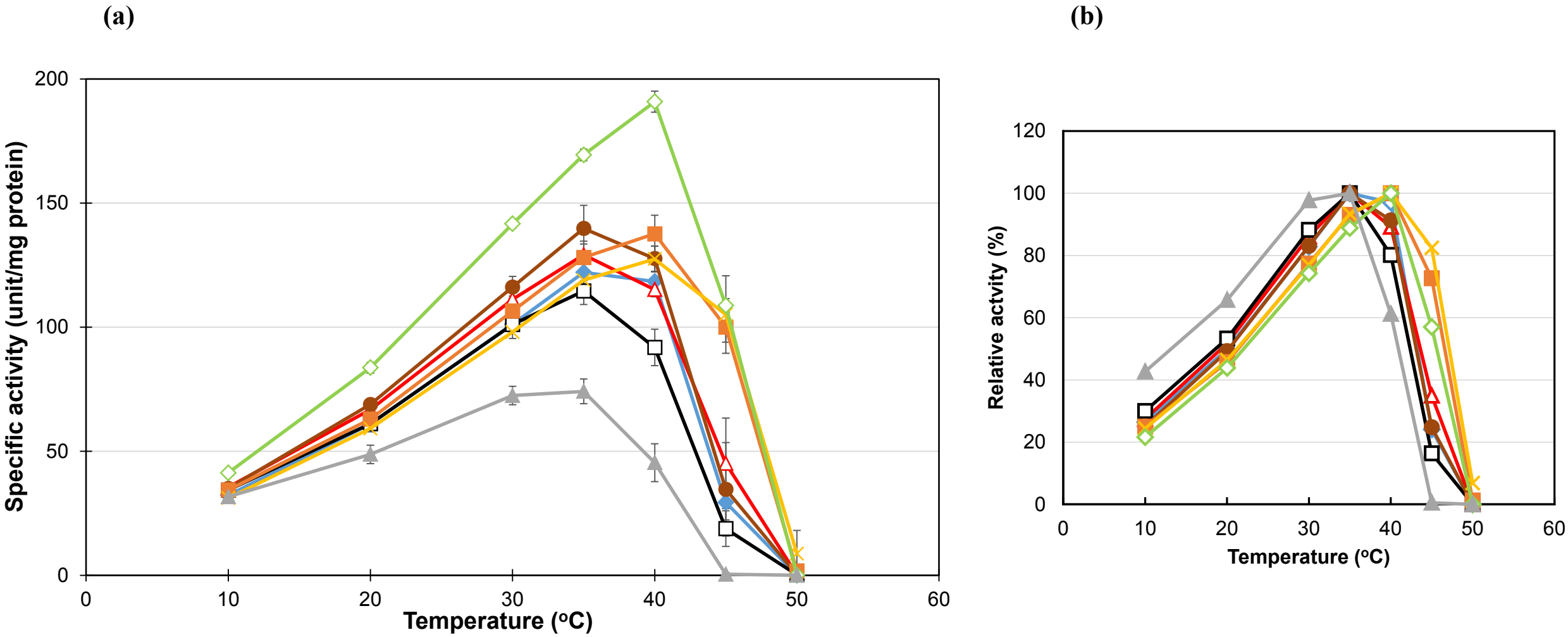
(a)
(b)
Specific activity (unit/mg protein)
Temperature (°C)
Relative actvity (%)
Temperature (°C)

Fig. 2

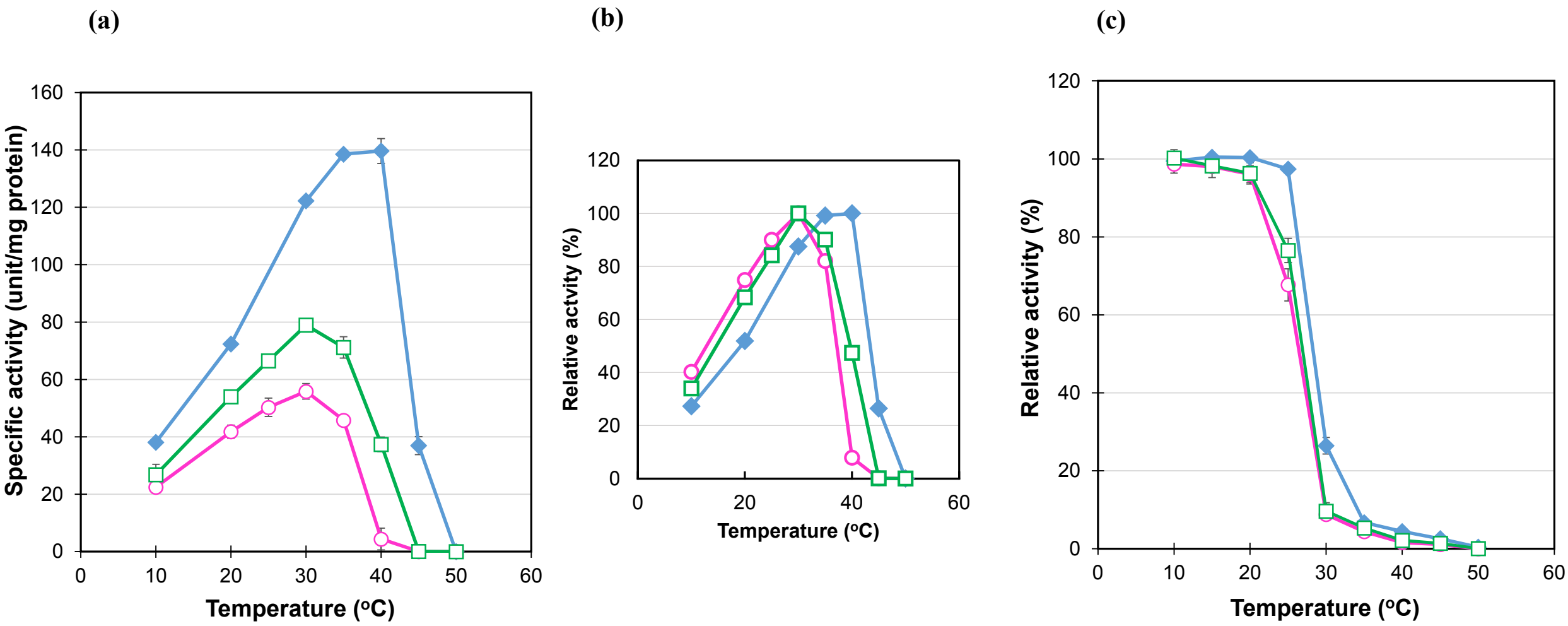
(a)
(b)
(c)
Specific activity (unit/mg protein)
Relative actvity (%)
Relative activity (%)
Temperature (°C)
Temperature (°C)
Temperature (°C)
0
20
40
60
80
100
120
140
160
0
10
20
30
40
50
60

Fig. 3

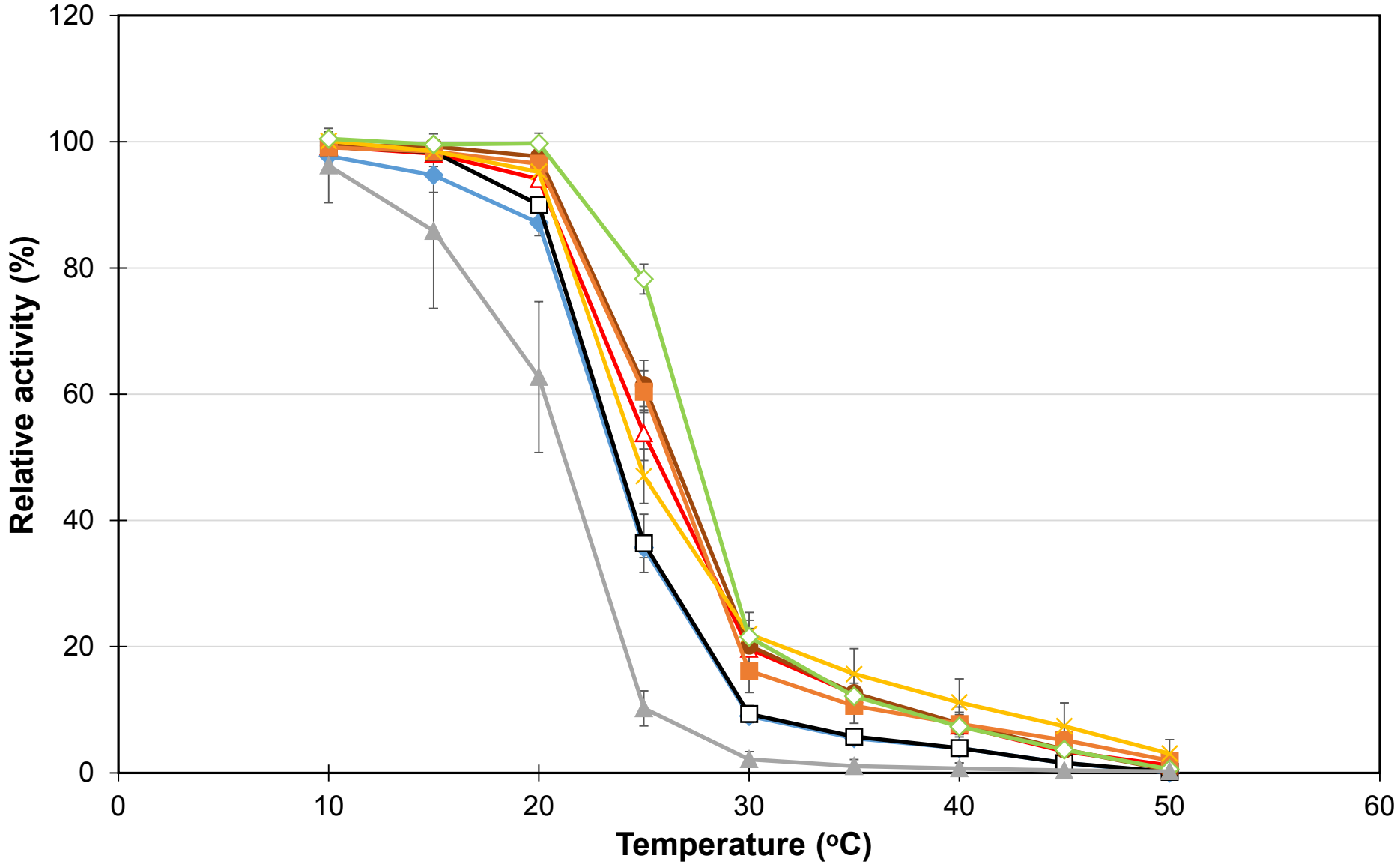
120
100
80
60
40
20
0
Relative activity (%)
0
10
20
30
40
50
60
Temperature (°C)

Fig. 4

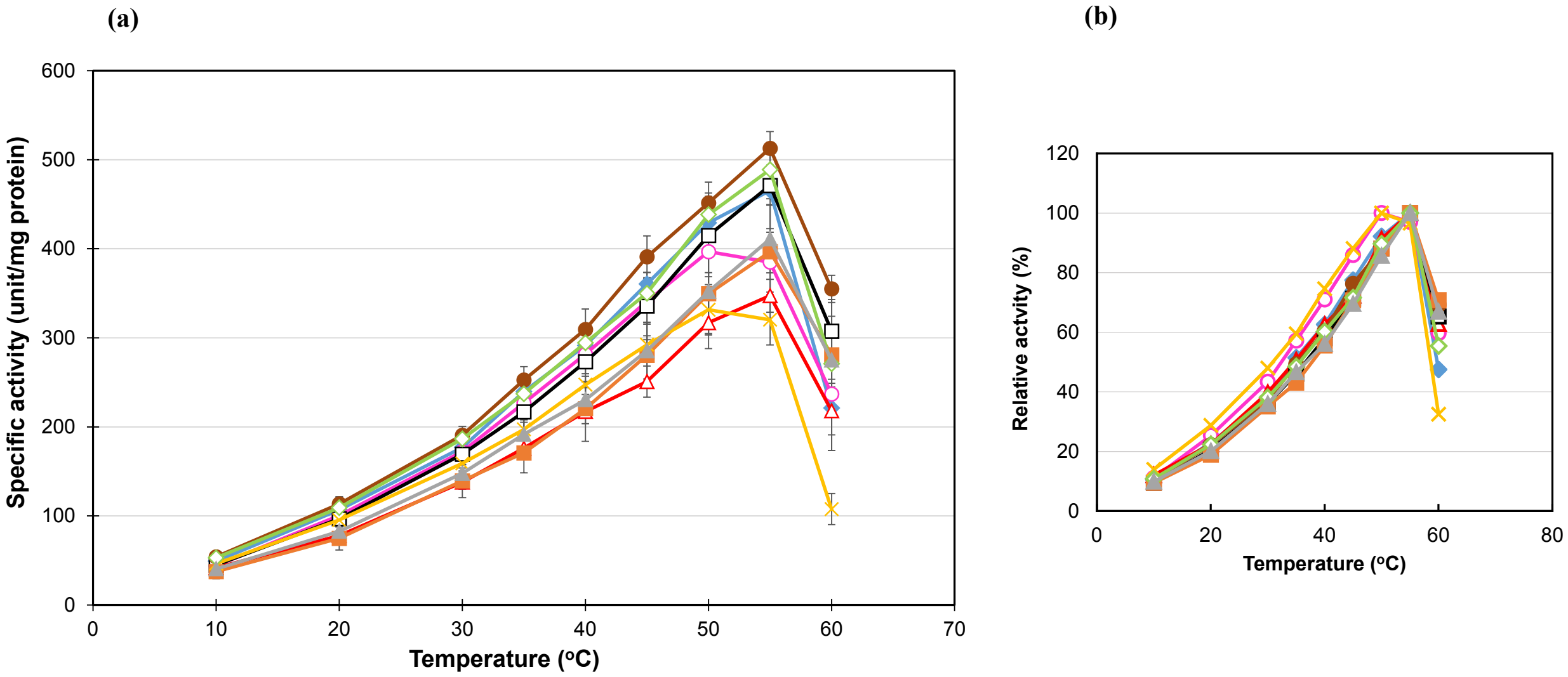
(a)
(b)
Specific activity (unit/mg protein)
Temperature (°C)
Relative actvity (%)
Temperature (°C)

Fig. 5

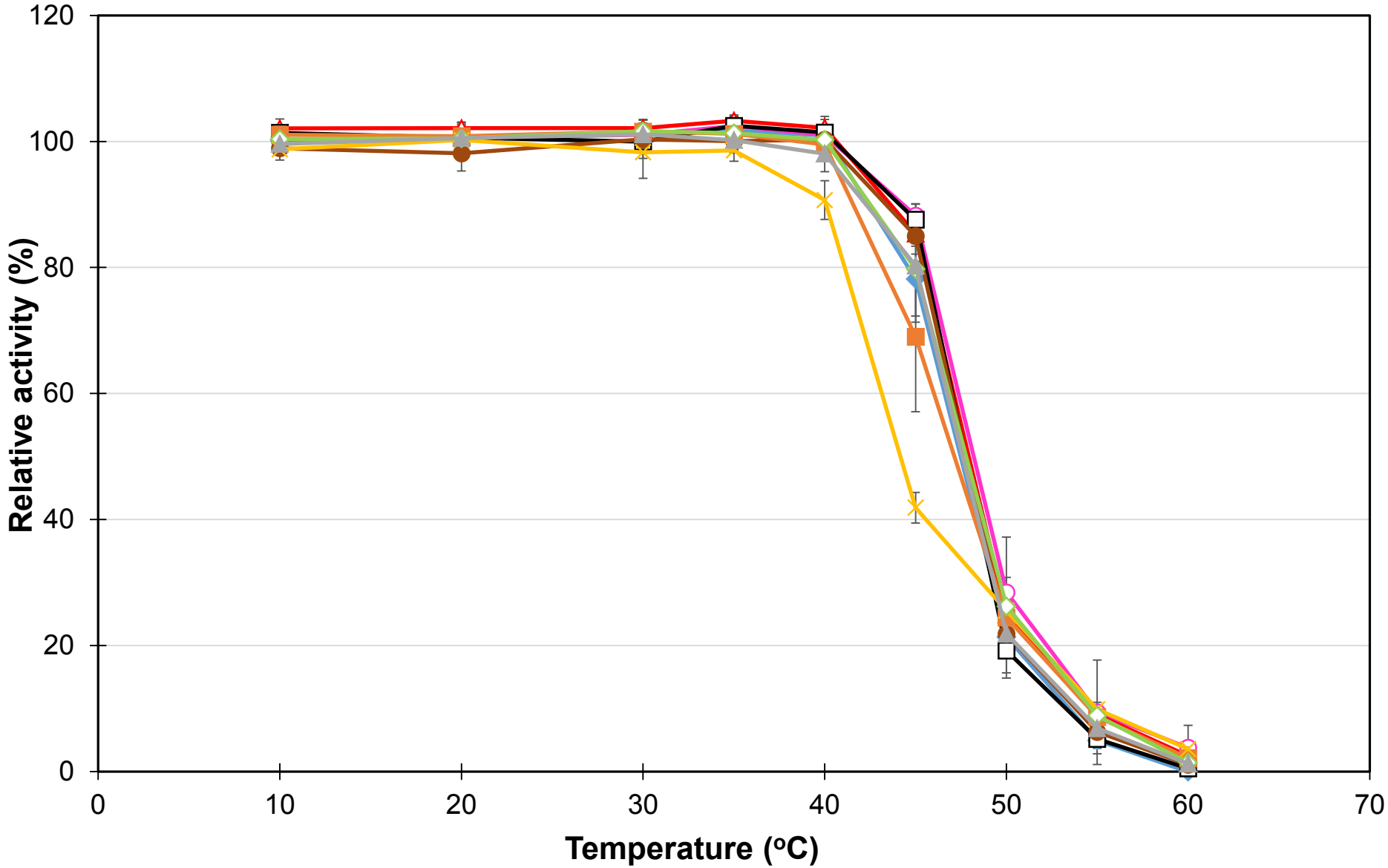
120
100
80
60
40
20
0
Relative activity (%)
0
10
20
30
40
50
60
70
Temperature (°C)

Fig. 6

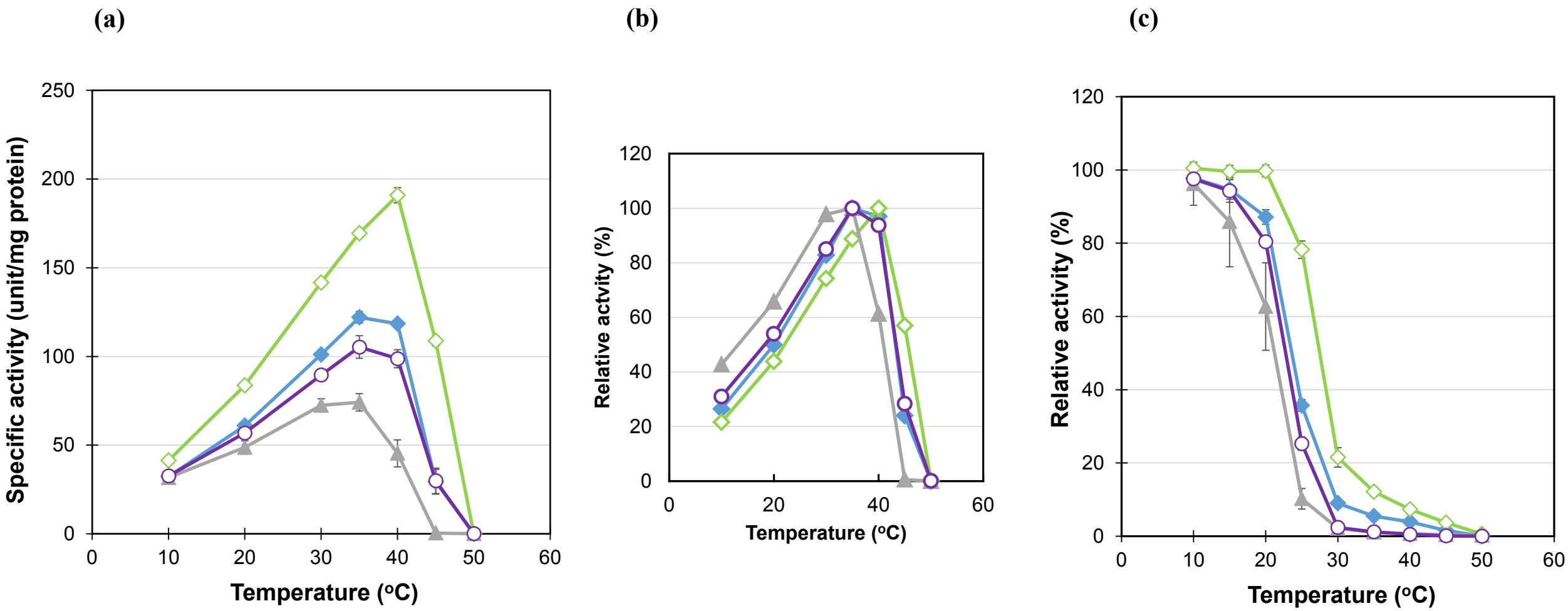
(a)
(b)
(c)
Specific activity (unit/mg protein)
Relative actvity (%)
Relative activity (%)
Temperature (°C)
Temperature (°C)
Temperature (°C)

Fig. 7

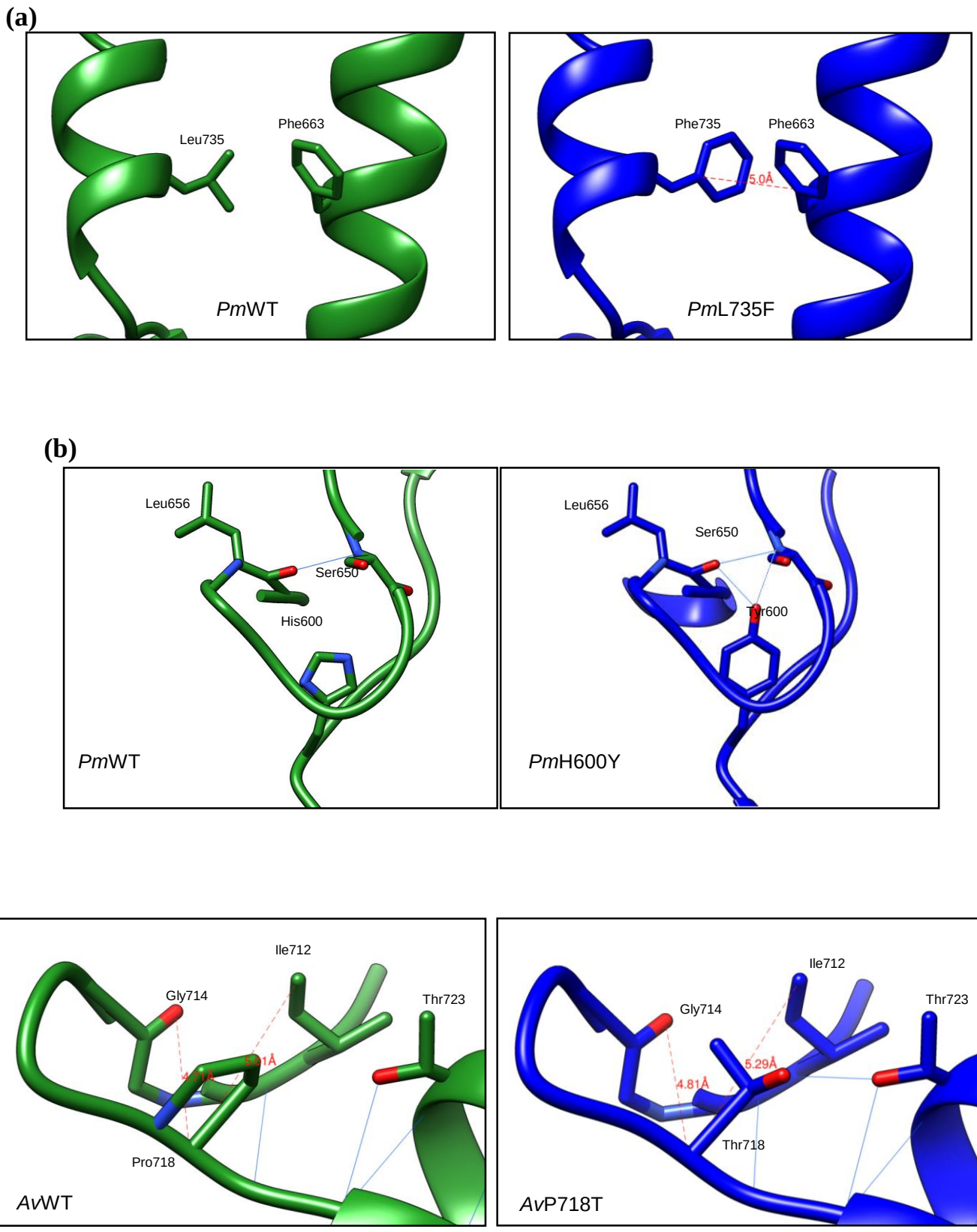
(a)
Leu735
Phe663
PmWT
Phe735
Phe663
5.0Å
PmL735F
(b)
Leu656
Ser650
His600
PmWT
Leu656
Ser650
Tyr600
PmH600Y
(c)
Ile712
Gly714
Thr723
5.01Å
4.81Å
Pro718
AvWT
Ile712
Gly714
Thr723
5.29Å
4.81Å
Thr718
AvP718T

Fig. 8

Table 1 Specific activities at 10ºC and optimum temperatures of the wild-type and mutated *Pm*IDHs, the optimum temperatures for activities and the $t_{½}$ values

	Specific activity (unit/mg protein) at		T_{opt}	$t_{½}$ value
	10ºC	Optimum temperature	(ºC)	(ºC)
*Pm*WT	32.25 ± 1.17	122.1 ± 3.29*	35 – 40	23.6
*Pm*A626P	35.48 ± 1.05	129.1 ± 5.55	35	25.6
*Pm*M667L	34.33 ± 0.48	114.6 ± 5.44	35	23.7
*Pm*T678E	34.97 ± 1.56	139.8 ± 9.34	35	26.4
*Pm*A711P	34.39 ± 2.11	137.6 ± 7.50	40	26.2
*Pm*T720P	31.12 ± 0.91	127.4 ± 5.22	40	24.7
*Pm*L735F	41.28 ± 1.45	190.9 ± 4.25	40	27.5
*Pm*N741P	31.62 ± 1.50	74.12 ± 4.94*	30 – 35	21.2
*Pm*L735FN741P	32.61 ± 1.04	105.3 ± 6.36*	35 – 40	22.7
*Pm*WT	38.13 ± 0.51	139.6 ± 4.33**	35 – 40	28.3
*Pm*H600Y	22.48 ± 1.48	55.85 ± 2.73	30	26.5
*Pm*H600YL735F	26.84 ± 3.59	78.98 ± 2.17	30	27

The lower three IDHs were diluted with the buffer containing 10% glycerol before the enzyme assay (see “Materials and methods”).

* The specific activities at 35ºC are shown.

** The specific activity at 40ºC is shown.

Table 2 Specific activities at 10ºC and optimum temperatures of the wild-type and mutated *Av*IDHs, optimum temperatures for activities and the $t_{½}$ values

	Specific activity (unit/mg protein) at		T_{opt}	$t_{½}$ value
	10ºC	Optimum temperature	(ºC)	(ºC)
*Av*WT	49.09 ± 1.18	465.5 ± 9.27	55	47.5
*Av*Y598H	44.01 ± 2.88	396.7 ± 28.0*	50 – 55	48.2
*Av*P624A	41.80 ± 3.03	347.2 ± 18.4	55	47.9
*Av*L665M	44.75 ± 7.65	471.0 ± 48.4	55	47.7
*Av*E676T	54.01 ± 2.87	512.7 ± 18.8	55	47.8
*Av*P709A	37.45 ± 8.17	396.6 ± 52.9	55	47.1
*Av*P718T	46.36 ± 0.96	331.5 ± 28.3*	50 – 55	44.2
*Av*F733L	52.86 ± 1.54	488.8 ± 23.6	55	47.8
*Av*P739N	40.50 ± 3.35	410.9 ± 38.0	55	47.6

* The specific activities at 50ºC are shown.

Table 3 Kinetic parameters of the wild-type and mutated *Pm*IDHs and *Av*IDHs at 20ºC

	K_m for isocitrate (μM)	k_{cat} (s^{-1})	$k_{cat}/K_m \times 10^5$ ($s^{-1}M^{-1}$)
*Pm*WT	33.53±1.54	102.98±5.82	30.86
*Pm*L735F	28.14±0.90	136.56±7.36	48.49
*Pm*N741P	62.04±8.27	100.53±7.11	16.34
*Pm*L735FN741P	46.37±4.47	102.94±3.19	22.34
*Av*WT	12.58±0.32	159.48±2.39	126.90
*Av*P718T	8.74±0.72	120.39±0.04	138.67
*Pm*WT	36.58±3.03	103.97±7.85	28.44
*Pm*H600Y	108.44±5.90	61.18±0.32	5.66
*Pm*H600YL735F	83.53±3.94	88.09±0.45	10.57

The lower three IDHs were diluted with the buffer containing 10% glycerol before the enzyme assay (see “Materials and methods”).

Supplementary Table S1. Oligonucleotides used in site-directed mutagenesis of *Pm*IDH

	Category of primer	Primer name	Nucleotide sequence (5' to 3')
For *Pm*IDH mutagenesis	Forward primer A	P. marina-M Histag-F	GCGCGGATCCGACCGATAAATCTGCA
	Reverse primer B	H600Y-r	GAATCCCAACGTAAATAGTTTTCTTCAAC
		A626P-r	GCCAATACAACCGCTTGTGGGTTATTTG
		M667L-r	CAGCCCAGTACAGAGCAAGGTAGAAATG
		T678E-r	GTAGTGCCGCATCTTCTGTTTGTGCTGC
		A711P-r	CCTAAATCAACCGGAACACCCTGTGCACC
		T720P-r	CACTTTGTCTTGGTCTGGATGGAAGTAACC
		L735F-r	GCTAATGCTGCATTGAATGTTTTACTTGG
	Forward primer C	H600Y-f	GTTGAAGAAAACTATTTACGTTGGGATTC
		A626P-f	CAAATAACCCACAAGCGGTTGTATTGGC
		M667L-f	CATTTCTACCTTGCTCTGTACTGGGCTG
		T678E-f	GCAGCACAAACAGAAGATGCGGCACTAC
		A711P-f	GGTGCACAGGGTGTTCCGGTTGATTTAGG
		T720P-f	GGTTACTTCCATCCAGACCAAGACAAAGTG
		L735F-f	CCAAGTAAAACATTCAATGCAGCATTAGC
	Reverse primer D	P. marina-M Histag-R	GCGCGAGCTCTTAAGTTTAGTATTATC
	Reverse primer D'	N741P-r	GCGCGCGAGCTCTTAAATGGGAGCTAATGC

Underlined letters indicate additional bases for introducing the digestion sites for *Bam*HI and *Sac*I (letters in gray boxes).

Supplementary Table S2 Oligonucleotides used in site-directed mutagenesis of *Av*IDH

	Category of primer	Primer name	Nucleotide sequence (5' to 3')
For *Av*IDH mutagenesis	Forward primer E	AF0	GCGCGGATCCGTCCACACCGAAGATTATC
	Reverse primer F	Y598H-r	GAATCCCAACGCAGGTGACCTTCCTCGAG
		P624A-r	GGACAAGCGCTTTCGCGTTCTTGTAGGC
		L665M-r	CTGGGCCCAGTACATTGCCAAGTAGAAG
		E676T-r	CAGTTCCTTGTCCGTGGTTTGCGCTGC
		P709A-r	CAGCGATATCCACAGCCTTGCCTTGGGC
		P718T-r	GGTCAGGTCGGTATTCGTATGGTAGTAGCC
		F733L-r	GTGCCAGAGCCGCGTTTAAAGTAGCGCTC
	Forward primer G	Y598H-f	CTCGAGGAAGGTCACCTGCGTTGGGATTC
		P624A-f	GCCTACAAGAACGCGAAAGCGCTTGTCC
		L665M-f	CTTCTACTTGGCAATGTACTGGGCCCAG
		E676T-f	GCAGCGCAAACCACGGACAAGGAACTG
		P709A-f	GCCCAAGGCAAGGCTGTGGATATCGCTG
		P718T-f	GGCTACTACCATACGAATACCGACCTGACC
		F733L-f	GAGCGCTACTTTAAACGCGGCTCTGGCAC
	Reverse primer H	AR0	GCGCGAGCTCTTATGCAAGAGGTGCCAG
	Reverse primer H'	P739N-r	GCGCGCGAGCTCTTATGCAAGATTTGCCAG

Underlined letters indicate additional bases for introducing the digestion sites for *Bam*HI and *Sac*I (letters in gray boxes).

Supplementary Table S3 Cycle conditions for PCR in site-directed mutagenesis of *Pm*IDH

		Mutation	Annealing temperature (˚C)	Extension time (s)
For *Pm*IDH mutagenesis	first PCR	H600Y	46	60
		A626P	50	60
		M667L	51	66
		T678E	52	63
		A711P	52	67
		T720P	52	68
		L735F	47	70
		H600YL735F	47	70
	second PCR	H600Y	46	20
		A626P	47	15
		M667L	47	15
		T678E	47	12
		A711P	47	7
		T720P	47	8
		L735F	47	10
		H600YL735F	47	10
	third PCR	H600Y	47	72
		A626P	47	72
		M667L	47	72
		T678E	47	72
		A711P	47	70
		T720P	47	72
		L735F	47	72
		N741P	52	66
		H600YL735F	47	72
		H600YN741P	52	72
		L735FN741P	52	72
		H600YL735FN741P	52	72

After denaturation at 94˚C for 15 s, annealing at the indicated temperatures for 30 s and extension at 68˚C for the indicated times was carried out for 30 cycles.

Supplementary Table S4 Cycle conditions for PCR in site-directed mutagenesis of *Av*IDH

		Mutation	Annealing temperature (˚C)	Extension time (s)
For *Av*IDH mutagenesis	first PCR	Y598H	55.6	60
		P624A	54	70
		L665M	53	66
		E676T	54	63
		P709A	65	180
		P718T	54	68
		F733L	55	70
	second PCR	Y598H	55.6	20
		P624A	54	15
		L665M	55	15
		E676T	54	12
		P709A	65	30
		P718T	54	8
		F733L	50	10
	third PCR	Y598H	55	72
		P624A	55	70
		L665M	55	72
		E676T	55	72
		P709A	65	180
		P718T	55	72
		F733L	55	72
		P739N	55	66

After denaturation at 94˚C for 15 s, annealing at the indicated temperatures for 30 s and extension at 68˚C for the indicated times was carried out for 30 cycles.

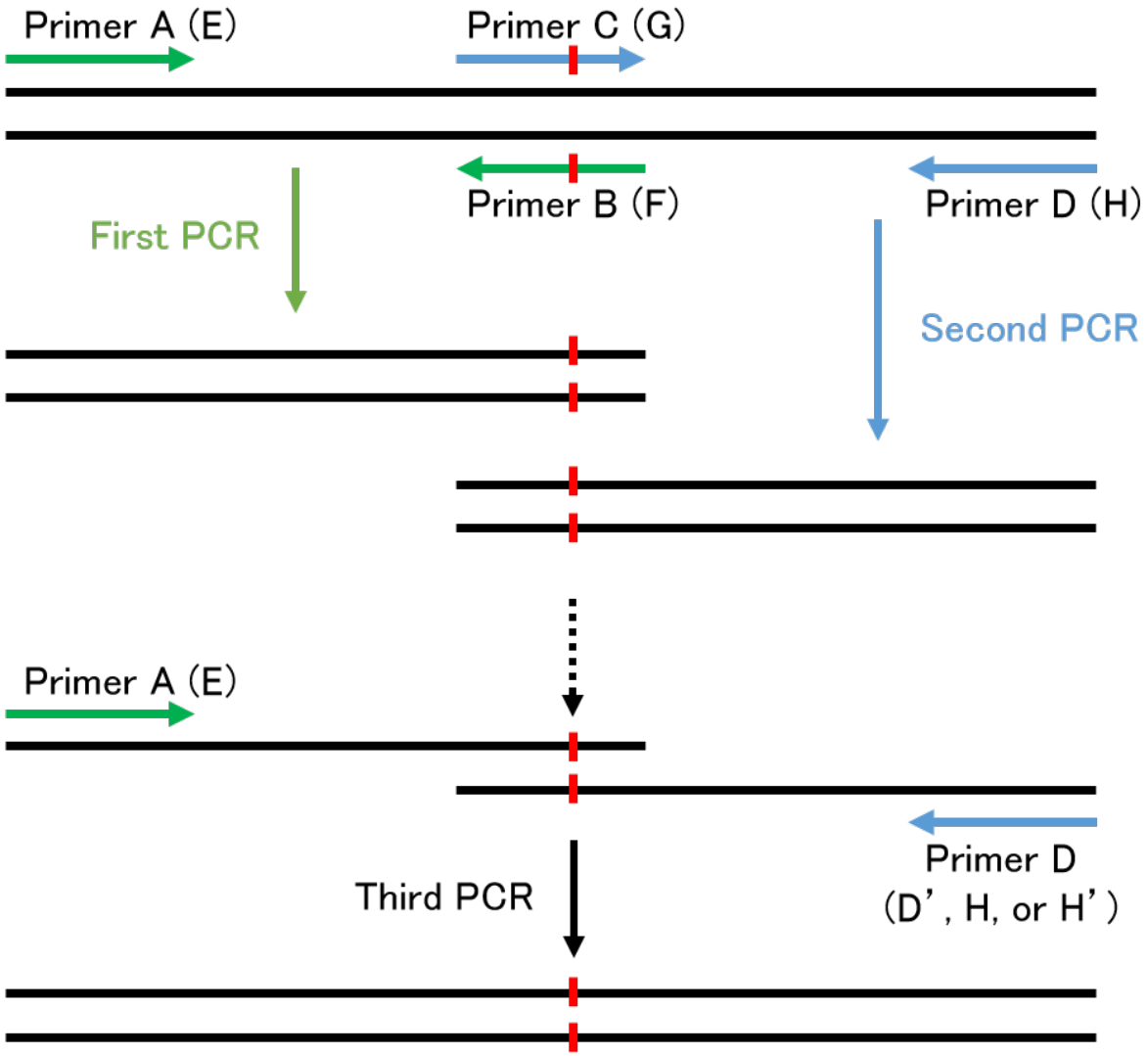

Supplementary Fig. S1 Schematic diagram of site-directed mutagenesis. Red bars indicate the positions of the substituted amino acid residues.

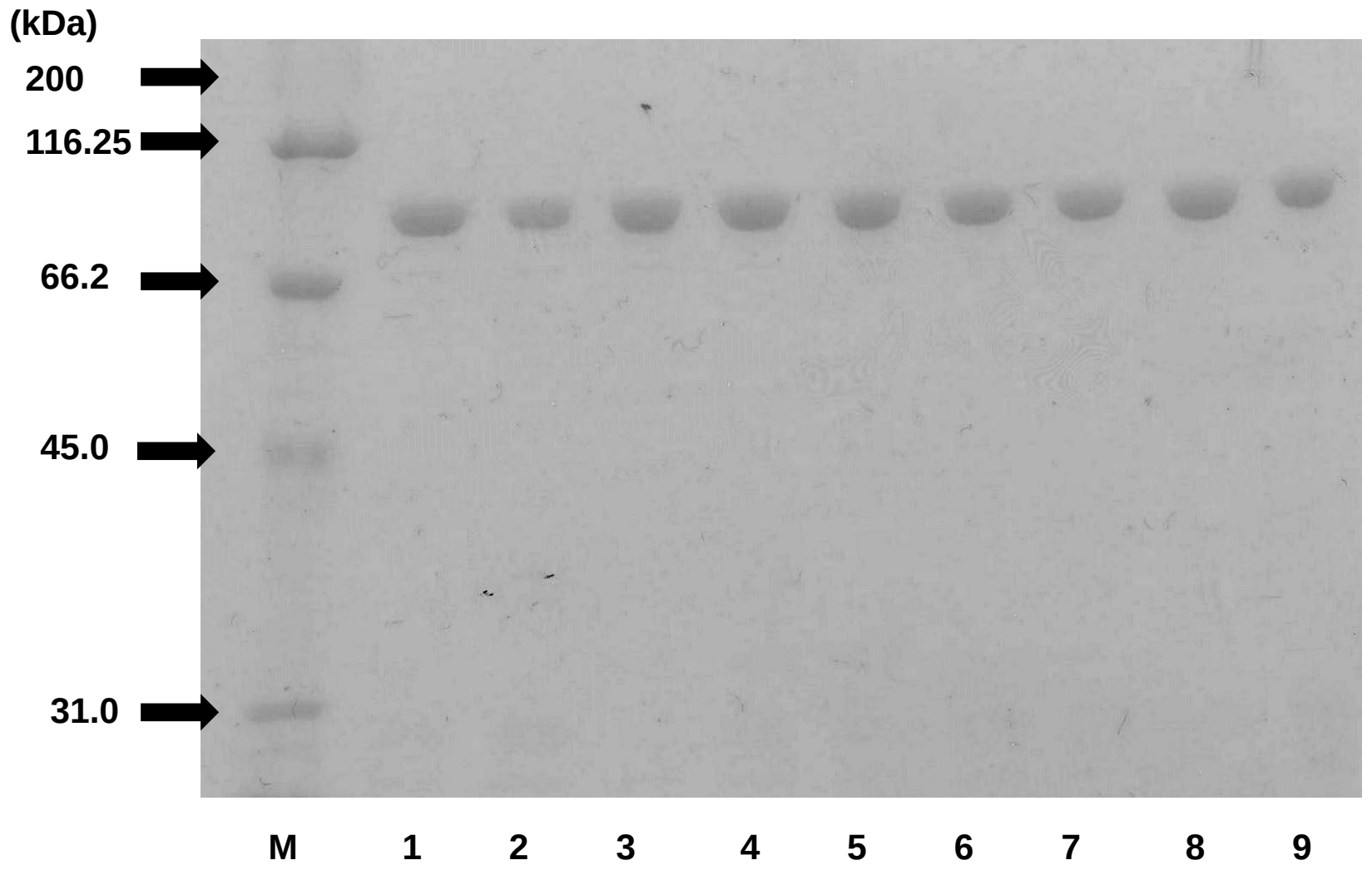

Supplementary Fig. S2 SDS-PAGE of the wild-type and mutated *Pm*IDHs. Three μg of protein was applied to each lane. Lane M, marker proteins; lane 1, wild-type *Pm*IDH; lane 2, *Pm*H600Y; lane 3, *Pm*A626P; lane 4, *Pm*M667L; lane 5, *Pm*T678E; lane 6, *Pm*A711P; lane 7, *Pm*T720P; lane 8, *Pm*L735F; lane 9, *Pm*N741P.

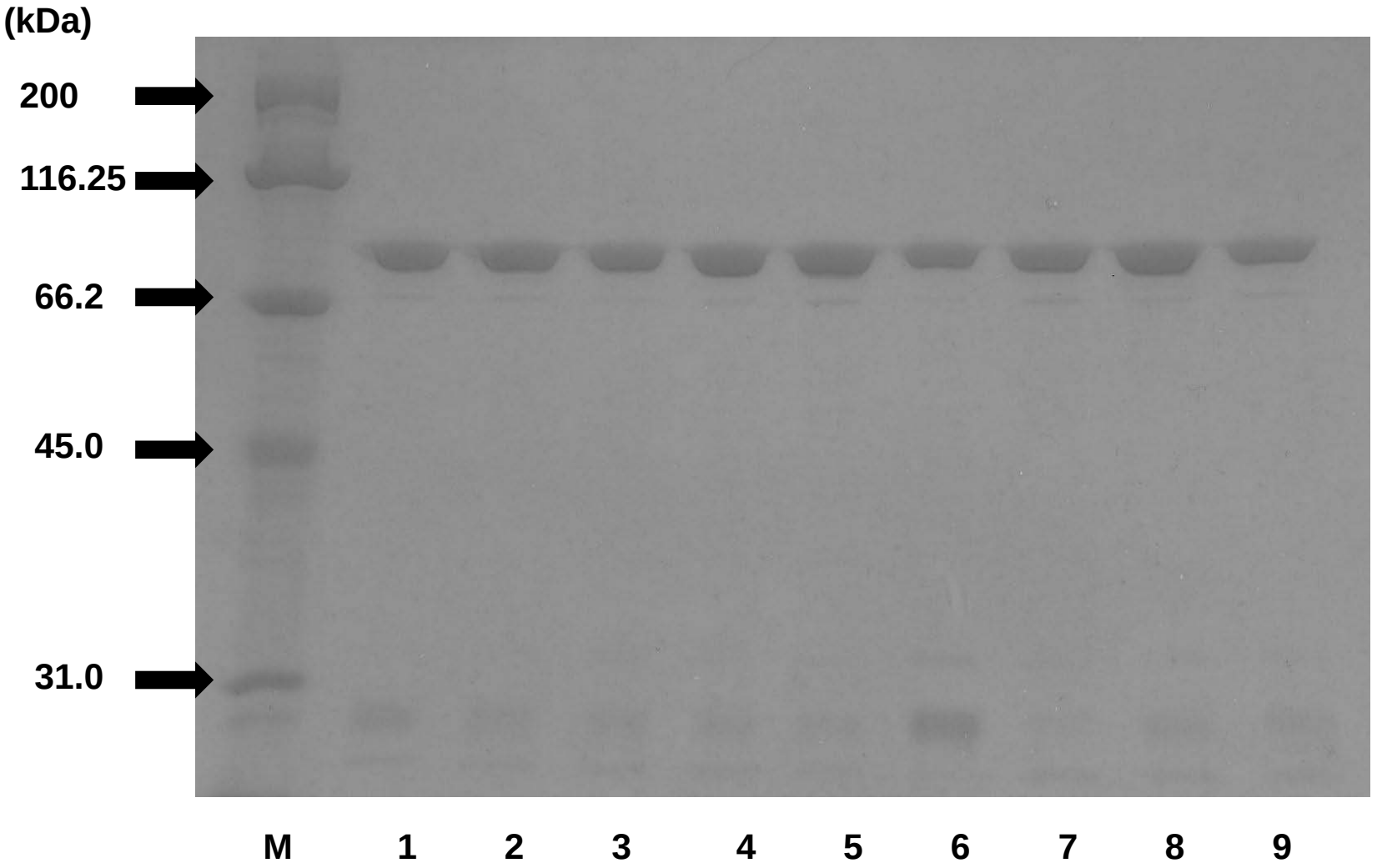

Supplementary Fig. S3 SDS-PAGE of the wild-type and mutated *Av*IDHs. Three μg of protein was applied to each lane. Lane M, marker proteins; lane 1, wild-type *Av*IDH; lane 2, *Av*Y598H; lane 3, *Av*P624A; lane 4, *Av*L665M; lane 5, *Av*E676T; lane 6, *Av*P709A; lane 7, *Av*P718T; lane 8, *Av*F733L; lane 9, *Av*P739N.

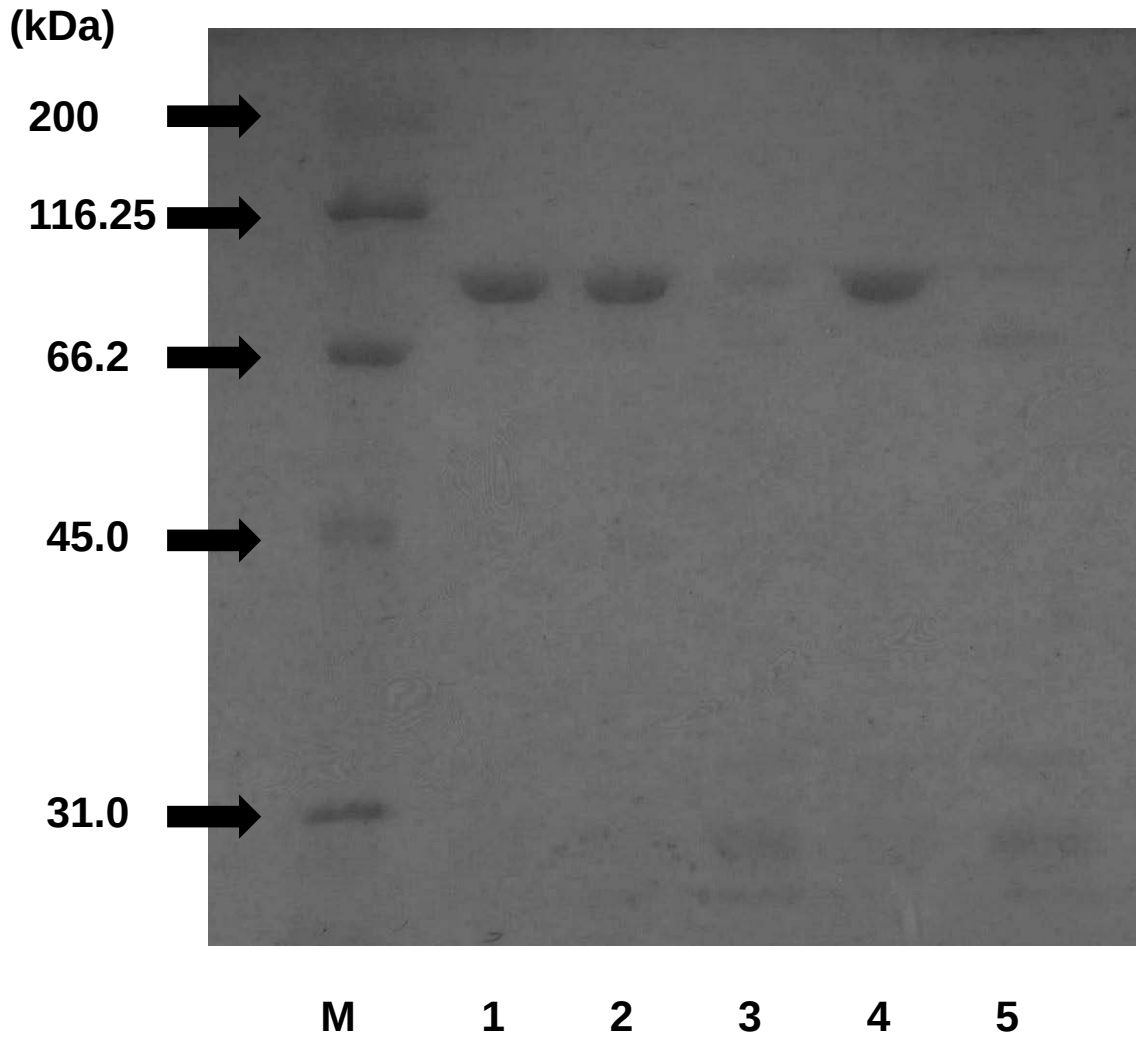

Supplementary Fig. S4 SDS-PAGE of the wild-type *Pm*IDH and multiple mutants. Three μg of protein was applied to each lane. Lane M, marker proteins; lane 1, wild-type *Pm*IDH; lane 2, *Pm*H600YL735F; lane 3, *Pm*H600YN741P; lane 4, *Pm*L735FN741P; lane 5, *Pm*H600YL735FN741P.